Energy Geotechnics – Wuttke, Bauer & Sánchez (Eds)
© 2016 Taylor & Francis Group, London, ISBN 978-1-138-03299-6

Thermo-mechanical behaviour of energy pile in underground railway construction site

M. Adinolfi, A. Mauro, R.M.S. Maiorano, N. Massarotti & S. Aversa
Università Degli Studi di Napoli "Parthenope", Napoli, Italy

ABSTRACT: The use of geothermal pile foundations is an environmental friendly way to extract/storage energy from/in the ground. The operating principle of these innovative structures is based on energy transfer between the ground and the fluid flowing inside the probes inserted in the pile, in order to feed heat pumps dedicated to buildings heating and cooling. Nevertheless, very limited installations are recorded in Italy, and only few information are available regarding the impact of thermal processes on the structural performance of energy piles. In the present work, the geo-energy research group has analysed the thermo-hydro-mechanical behaviour of an energy pile installed in pyroclastic soils and rocks, as an element of a sheet pile wall. The developed model, solved numerically by using finite elements, is then used to forecast the behaviour of an actual pile subjected to thermo-mechanical loads and to design a proper experimental campaign in the underground railway construction site of Piazza Municipio in Napoli, Italy.

The multi-pile experimental set-up is equipped with fibre optic sensors system that allows the evaluation of strains and temperature distributions along the piles during cooling and heating processes. Once the measurements will be available, the developed model will be verified and validated against on field experiments.

1 INTRODUCTION

In recent times, the diffusion of geothermal pile foundations to extract/store up energy from/in the ground is rapidly growing (Brandl 2006, Amis et al. 2014), also for its economic advantages due to the reduction of installation costs with respect to traditional geothermal probes. The operating principle of these innovative structures is based on energy transfer between the ground and the fluid flowing inside probes inserted in the pile, in order to feed heat pumps dedicated to buildings heating and cooling (Brandl 2006). Experimental tests have been conducted (Laloui et al. 2006, Bourne-Webb et al. 2009) on energy piles, showing that the thermally induced axial stress inside the pile strictly depends on the end-restraint provided by the overlying structure, thermal loads and the properties of the foundation material (Amatya et al. 2012). Many numerical approaches are available in the literature. Related to heat and fluid flow through porous media is presented a novel method in Carotenuto et al. 2012 and a comprehensive review of the developed models for thermo-fluid dynamic phenomena in low enthalpy geothermal energy systems is proposed in Carotenuto et al. 2016. Concerning the coupled phenomena thermal, hydraulic and mechanical (THM) several models are available about effects on single energy pile and the surrounding soil (Laloui et al. 2006, Salciarini et al. 2012, Suryatriyastuti et al. 2012) and piles group (Dupray et al. 2014, Jeong et al. 2014, Salciarini et al. 2015). The aims of this work are to describe the experimental set-up and to propose a proper finite element THM model in poroelastic media allowing the simulation of complex soil-structure interaction phenomena for thermo-active piles, in order to evaluate the performance of the geothermal pile in the investigated area.

2 EXPERIMENTAL SET UP

2.1 *The site*

The experimental set-up has been realized in the construction site of the underground station of Piazza Municipio in Napoli, Italy. The train platform of the original project is located at 13.5 m below the ground level. A sheet pile wall is realized by means of forty-five bored piles (800 mm nominal diameter), at a inter-axis distance of 1.10 m, and six of them have been used for the present set-up, by incorporating, in the concrete casting, the geothermal probes made of High Density PolyEthylene (HDPE). The total length of piles to support the excavation of 6 m is equal to 11.40 m. The average normal load on each pile is smaller than 1200 kN. The tested elements are located within the sheet-pile retaining wall. The HDPE probes (32 mm nominal diameter) were fixed to the pile reinforcing cage (Fig. 1). Different probes configurations have been provided in order to check their performances: spiral, double and triple U-shape.

2.2 *The instrumentation*

The reinforcement cage (details available in Figure 1) has been used also to support Optic Fiber Sensors

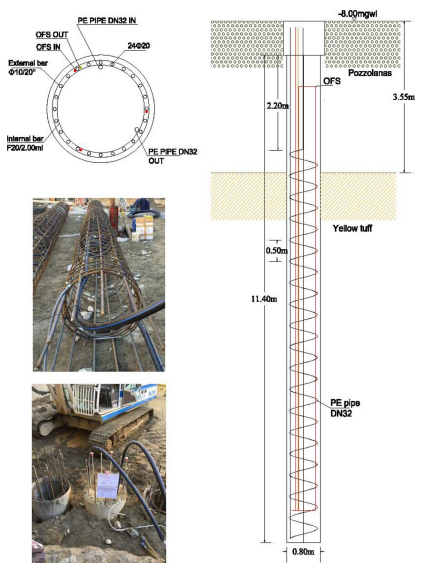

Figure 1. Experimental set up details: typical section of equipped pile; pictures of set-up distribution of OFS cables and spiral probes before and after concrete casting; pile section with geometric and ground features.

(OFS), for strain and temperature measurements. In particular, about 180 m of OFS cables were installed in three of the six probes-equipped piles. Two methods of installation, one with the cable anchored continuously along the length of the reinforcement cage at regular steps and one with the cable strung between the top and bottom of the cage were used. As concerns strain measurements, three fibres, installed at 120° along the pile circumference, allow to derive the vectorial displacements of each pile section. The fourth optical cable was strung along the pile for distributed temperature measurements and a traditional temperature sensor was used to obtain a reference temperature value. The monitoring system is made up by an opto-electronic reading unit, including all the electronic and optical components and cables.

2.3 *Soil conditions*

The sheet pile wall is located inside a larger excavation with its top at a depth of 8.00 m below ground water level (gwl). Ground conditions, are typical for Neapolitan area: a superficial layer of granular pyroclastic products of volcanic activity called "pozzolanas" (3.55 m thick) overlies a lithified stratum of yellow tuff, at depth of 11.55 m below gwl, which extends for many meters under the piles toe. Since the water level is well above the top of the sheet pile wall, all the soils are considered as saturated (Fig. 1). The energy piles installation was undertaken within an active construction site. Therefore, the experimental campaign will be designed compatibly with all the other activities of the underground station. Moreover several additional in situ and laboratory tests will be realized to characterize the materials, including thermal conductivity and permeability tests on soil samples, integrity tests on the concrete, performance evaluation on heat exchangers and ground response tests.

3 THERMO-HYDRO-MECHANICAL MODEL

3.1 *Mathematical formulation*

A coupled thermo-hydro-mechanical model has been developed to simulate the behaviour of one of the piles of the experimental set-up during the preliminary tests, to be carried out before the soil beneath the sheet pile wall will be excavated. The governing equations reproducing the mechanical behaviour of the solid skeleton, the heat conduction phenomena and the hydraulic motion in the soils are solved. The model is based on the following assumptions: soils are modelled as isotropic and linear elastic materials (the applied mechanical loads are significantly smaller than the collapse values); displacements and deformations of the solid skeleton are small (linear kinematics); perfect contact between soil and pile is considered; hydrostatic pressures are neglected. Taking into account the previous assumptions, the applied equations are:

$$\nabla\boldsymbol{\sigma}+\mathbf{b}=\mathbf{0} \tag{1}$$

$$\boldsymbol{\sigma}=\mathbf{D}^{\mathbf{e}}\left(\boldsymbol{\varepsilon}-\boldsymbol{\varepsilon}^{\mathbf{T}}\right)-\alpha_B\cdot p\cdot\mathbf{I} \tag{2}$$

$$\boldsymbol{\varepsilon}^{\mathbf{T}}=1/3\cdot(\alpha_s\cdot\Delta T)\cdot\mathbf{1} \tag{3}$$

$$\mathbf{v}=-\mathbf{k}\cdot\nabla p \tag{4}$$

$$\rho\cdot\alpha_B\cdot div\frac{\partial e_{vol}}{\partial t}+S\cdot\rho\cdot\frac{\partial p}{\partial t}+\nabla(\rho\cdot\mathbf{v})-\rho\cdot\beta_{sw}\cdot\frac{\partial T}{\partial t}=0 \tag{5}$$

$$\beta_{sw}=(1-n)\cdot\alpha_s+n\cdot\alpha_{\mathrm{w}} \tag{6}$$

where $\boldsymbol{\sigma}$ = total stress tensor (positive if tensile); $\mathbf{b}$ = volume external force vector; p = pore water pressure increase (positive if compressive); α_B = Biot Willis coefficient of porous media; $\mathbf{D}^{\mathbf{e}}$ = elastic stiffness tensor; $\boldsymbol{\varepsilon}$ = strain tensor; $\boldsymbol{\varepsilon}^{\mathbf{T}}$ = thermal strain tensor; T = temperature; $\mathbf{1}$ = second order unit tensor; α_{s} = volumetric thermal expansion coefficient of the soil; α_{w} = water thermal expansion coefficient; $\mathbf{v}$ = Darcy velocity vector; ρ = soil density; $\mathbf{k}$ = permeability tensor; $\mathrm{e_{vol}}$ = volumetric strain; β_{sw} is thermal volumetric expansion coefficient of the bi-phase mass; and S = storage coefficient taking into account for porosity, permeability, Biot Willis coefficient of soils. Heat transfer in porous media, including conduction and convection phenomena, uses the following equation:

$$\left(\rho\cdot C_p\right)_{eq}\cdot\frac{\partial T}{\partial t}+\rho_w\cdot C_{p_w}\cdot\nabla(T\cdot\mathbf{v})-\boldsymbol{\lambda}_{\mathbf{eff}}\cdot\nabla^2T=0 \tag{7}$$

$$\left(\rho\cdot C_p\right)_{eq}=(1-n)\cdot\rho\cdot C_{p_p}+n\cdot\rho_w\cdot C_{p_w} \tag{8}$$

where n = porosity of soils; ρ_{w} = water density; $\boldsymbol{\lambda}_{\mathbf{eff}}$ = thermal conductivity tensor of the soil; C_{ps} = solid skeleton thermal capacity and C_{pw} = water thermal capacity.

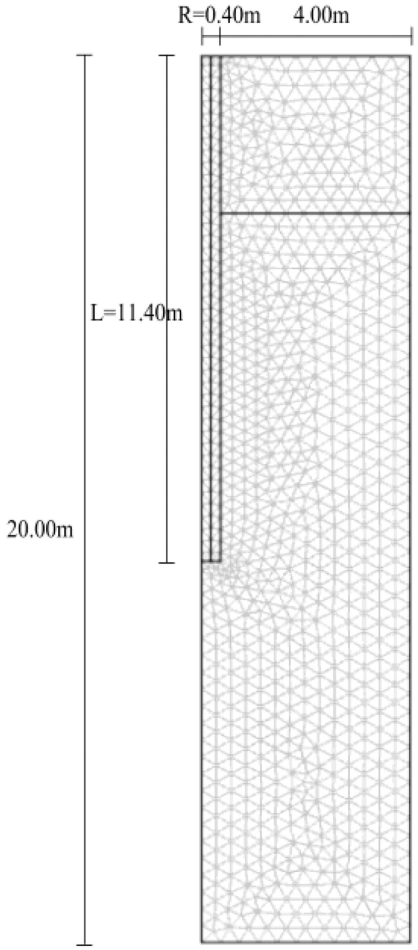

Figure 2. Axial-symmetric model region.

3.2 *FEM analysis*

The time-dependent numerical model has been implemented and solved by using the finite elements code Comsol Multiphysics version 4.3. The 2D model region, in the axial symmetric system, has a width of 4.00 m and a length of 20.00 m (Fig. 2).

The mechanical Boundary Conditions (BCs) are: fixed constraints at the bottom and roller condition on the side. The thermal BCs are: constant temperature on the heat exchanger, adiabatic conditions on all external boundaries. The hydraulic BCs are: no flow on the right and bottom boundaries and zero pressure on the top. Initial stress conditions are derived from the results obtained from steady-state simulations accounting for only gravity effects.

The model has been validated against experimental data available in the literature (Bourne-Webb et al. 2009). The geometric features are shown in Figures 1–2, and the material properties, taken from the literature (Viggiani & Rippa 1998; Aversa et al. 2013; Aversa & Evangelista 1993; Colombo 2010; Mottana & Campolunghi 2010; Bourne-Webb et al. 2009; Laloui et al. 2006) are reported in Table 1.

Table 1. Thermal, hydraulic and mechanical properties of soils.

Tuff		
Density (ρ)	17	[kN/m^3]
Young modulus (E)	1500	[MPa]
Poisson modulus (ν)	0.3	[–]
Thermal expansion (α_s)	4×10^{-5}	[K^{-1}]
Thermal conductivity (λ_{eff})	1.48	[W m^{-1}K^{-1}]
Thermal capacity (Cp)	850	[J kg^{-1}K^{-1}]
Permeability (k)	4×10^{-5}	[m/s]
Porosity (n)	0.550	[–]
Pozzolanas		
Density (ρ)	17	[kN/m^3]
Young modulus (E)	520	[MPa]
Poisson modulus (ν)	0.3	[–]
Thermal expansion (α_s)	4×10^{-5}	[K^{-1}]
Thermal conductivity (λ_{eff})	2.30	[W m^{-1}K^{-1}]
Thermal capacity (Cp)	800	[J kg^{-1}K^{-1}]
Permeability (k)	1×10^{-6}	[m/s]
Porosity (n)	0.525	[–]
Concrete		
Density (ρ)	17	[kN/m^3]
Young modulus (E)	40	[GPa]
Poisson modulus (ν)	0.2	[–]
Thermal expansion (α_s)	8.5×10^{-6}	[K^{-1}]
Thermal conductivity (λ)	2.10	[W m^{-1}K^{-1}]
Thermal capacity (Cp)	800	[J kg^{-1}K^{-1}]

3.3 *Loads time histories*

The loading time history lasts 4 months operation and it includes two phases: the application of the mechanical load at the pile head and the application of a seasonally cyclic thermal load under constant mechanical load. The applied mechanical load is 1200 kN. The thermal load is due to the temperature of the injected fluid, supposed constant along the probes, according to the law presented in Figure 3a. The authors are aware that this is an approximation, but for the present scope is retained acceptable. During the first month only mechanical load is applied and temperature is equal to 16.9°C (ground reference temperature in Naples). During the cooling phase (winter mode), the inflow temperature in probes is set to the value of 7°C ($\Delta T = 9.9$°C) maintained for 30 days, then the temperature in the probes is kept constant and equal to the initial ground reference value during the third month. The increase from reference temperature to 35°C ($\Delta T = 18.1$°C) occurs during the last month (summer mode). The effects of only mechanical load (M) are appreciated at time t = 720 h whereas both effects of mechanical-cooling (C+M) thermal loads are present at time t = 1440 h and mechanical-heating

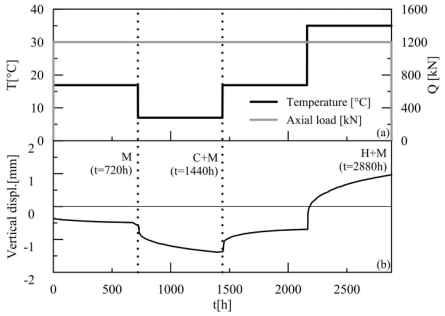

Figure 3. Time histories of applied thermal and mechanical loads (a); pile head vertical displacements (b).

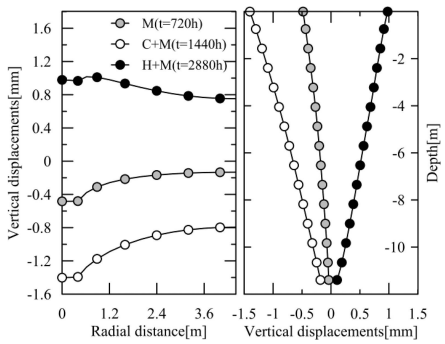

Figure 4. Pile and soil vertical displacements after mechanical and thermal loads at pile head.

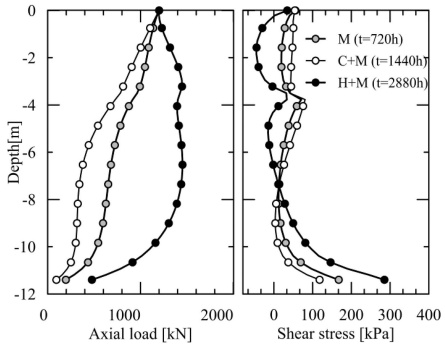

Figure 5. Axial load profiles and shear stress distribution along soil-pile interface after mechanical and thermal loads.

(H+M) thermal loads at time t = 2880 h (dotted lines in Figure 3a).

4 RESULTS

4.1 *Pile head and soil displacements*

Pile head displacements (Fig. 3b), produced by this thermo-mechanical loading cycle, are smaller than 1.4 mm and the maximum settlement is reached when both mechanical and cooling loads are applied. The analysis shows that the vertical displacement of the pile head follows the temperature changes.

Pile and surrounding soil displacements at the ground surface are plotted versus radial distance in the left side of Figure 4. The pile is subjected to the normal stresses of the soil at the toe, and to normal and tangential stresses on the shaft. The pile head under only mechanical load (t = 720 h) exhibits a maximum settlement of 0.48 mm and the effects of the axial load influence the surrounding soil with a compressive profile. When the thermal loads are added, the pile and the surrounding soil are more contracted during cooling phase according to their different thermal expansion coefficients and different temperatures, involving a settlement of 1.4 mm for head pile and 0.8 mm for surrounding soil. During the heating phase, the expansion of the pile leads to an uplift of 1.00 mm of its head, whereas the surrounding soil shows a decreasing path of upwards displacements versus radial distance.

The vertical displacements in the pile, along with depth, are plotted on the right side of Figure 4. Mechanical loads imply downward displacements (t = 720 h) maximum at pile head and minimum at the toe. At time t = 1440 h, the top of the pile tends to contract downward upon temperature decrease more than the toe. Contrariwise at time t = 2880 h, the pile tends to expand: the pile head moves upwards upon temperature increase, while the lower segment of the pile expands less reaching a null displacement at the toe.

4.2 *Axial loads*

Comparing the different plots of left side of Figure 5, it is possible to see, in terms of axial load, that the pile is obviously fully contracted at time t = 720 h when only mechanical load is applied. It results less compressed especially between 7.50 m and the pile's tip at the end of the subsequent cooling phase. An increase of the compressive load can be appreciated during heating phase with a consequent maximum load of 1450 kN due to the combined thermo-mechanical effects.

The distribution of shear stress along the interface is shown on the right side of Figure 5. The path follows a trend opposite to that of axial load in which at 3.55 m depth the change from pozzolanas to tuff soils in underlined by a cusp, which is directly correlated to soil strength and stiffness of layers. During the mechanical load the shear stresses act upward all over the length of the pile. In winter mode (C+M), due to different contractions between pile and soil, frictions mobilized along the upper part of pile increase whereas along the lower part of pile decrease. Inversely in summer mode (H+M), in the upper part of the pile the shear stresses act downward, while the lower part of pile has additional frictions mobilized. Moreover, it can be verified that when thermal loads are applied a neutral point appears, located at 6.70 m during heating process. It represents the point where the opposing soil shear stresses along the pile are balanced. Consequently, the compressional stress due to pile elongation and the associated soil resistance is maximized at the neutral point where themo-mechanical

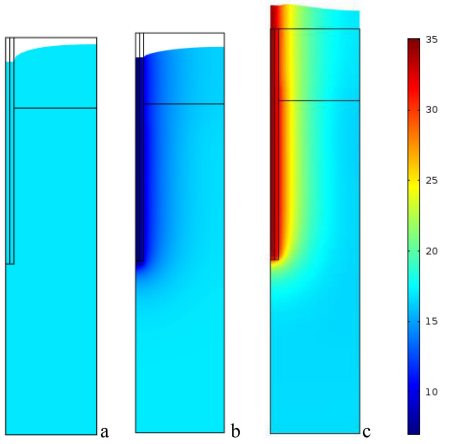

Figure 6. Temperature field (in °C) after the first month of analysis at t = 720 h (a), after cooling phase at t = 1440 h (b) and at the end of heating phase at t = 2880 h (c).

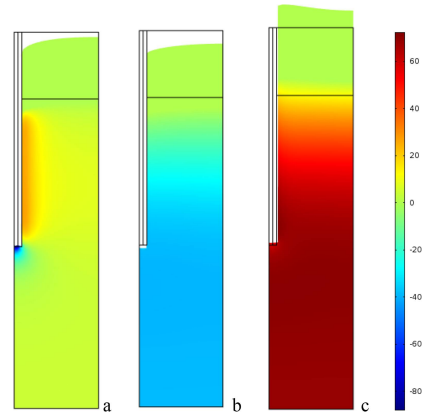

Figure 7. Pore water pressure field (in kPa) steps: thermal loading (cooling phase) application at t = 720 h (a), the end of cooling phase at t = 1440 h (b) and the end of heating phase at t = 2880 h (c).

shear stresses acting on the pile reverse from downward to upward along the pile length. The thermo-mechanical stress distribution would be symmetrical if the pile was free at both ends for an elastic soil with uniform stiffness throughout (Ozudogru et al. 2015).

4.3 *Thermal field*

The temperature field produced by the heat exchanger probes is shown in Figure 6 together with deformed axial-symmetric domain. The figure presents three significant temperature steps; the first one shows ground-pile system constant temperature at 16.9°C (Fig. 6a). During the cooling phase (Fig. 6b), the temperature ranges from 7°C inside the heat exchanger to 16.9°C in the ground. At the end of heating phase (Fig. 6c), the temperature ranges from 35°C inside probes to reaching ground initial temperature at boundaries of domain.

4.4 *Pore water pressure field*

Temperature changes around the pile induce changes through their effect on water and soil skeleton. In Figure 7a is plotted pressure field distribution at time t = 720 h.

Due to the cooling loading stage a reduction about −80 kPa of pore water pressure concentration (and increases the effective stress of the soil) is computed in the lower part of the pile whereas compressive pressures of 20 kPa is computed for the length pile in tuff, coherently with the differences in the soil hydraulic properties. At the end of cooling phase (t = 1440 h) the suction is dissipated and the residual induced pore water pressure variation is lower than 40 kPa at lower boundary of the domain (Fig. 7b). A reverse effect is produced when an increase in temperature expires an excess pore water pressure concentration at pile toe and tensile pressure of in the upper part of tuff layer. This increase in pore pressure can tend to cause water to flow away from the area, if the soil is sufficiently permeable that water flow is possible in a short time scale. At time t = 2880 h (Fig. 7c) excess of pore water pressure is not yet completely dissipated whereas residual pressure at this time is about 60 kPa.

5 CONCLUSIONS

Energy piles are foundations which support the loads of structure and provide thermal energy to the building as heat exchangers. They use the ground as energy source sink, successfully considered as an innovative environmentally friendly building's technology. In general, the amount of thermal energy exchanged depends on the type of soil, saturation degree, presence of groundwater flow, temperature of the ground and on the building energy needs. It is well known that additional thermal deformation and thermal stress that change the behaviour of material appear during cooling/heating processes.

This study is finalized to evaluate geotechnical effects and energy-related problems that can result from the use of energy pile under conventional temperatures in the tested site of the underground station of Piazza Municipio in Napoli, Italy. A preliminary numerical simulation is carried out with finite element method under mechanical and thermal loads for cooling and heating operation on a single pile in the construction site. The numerical results were in qualitative agreement with the experimental results of in situ tests at Lausanne and Lambeth College reported in literature. For the Piazza Municipio energy pile, the results show that:

- the pile head settlements are lower than 1.40 mm and its maximum elongation is of 1.00 mm. Due to low magnitude of these movements, there is slight influence in mechanical behaviour of the structure;

- when thermal loads are applied, the neutral point where the opposing soil shear stresses along the pile are balanced appears: its position strictly depends from pile constrains;
- cooling energy pile causes the thermal contraction of the pile, resulting in decreasing axial load along the pile. Inversely, heating energy pile causes an increase in axial load under combined thermo-mechanical loading reaching the maximum compressive value of 1450 kN. Typical problems for energy piles are: stresses may exceed the acceptable design stress, while large-amplitude strain cycles alter the magnitude and distribution of shaft friction mobilised between the pile and the soil (Laloui et al. 2006, Bourne-Webb et al. 2009). Obtained results, using a four-month time scale and conventional temperatures (7°C and 35°C), are far from collapse values;
- temperature distribution extends throughout surrounding soil for a radial distance of 3d (2.40 m) and for 4.50 m above pile's toe;
- the effect of the thermal behaviour of water in low permeability soil creates changes in the effective stresses of the soil. The proposed analysis shows that heating phase does not reduce significantly the effective stresses at pile toe but the knowledge of the soil permeability is necessary for the design of an energy pile foundation. Indeed huge reduction in effective stress could be detrimental to the stability of the building, due to a reduction in mobilized shaft friction along the piles.

Future developments will focus on the evaluation of the effects of variation of boundary conditions due to open excavations, required to accommodate the underground stations, and on model the whole retaining wall activating the group of equipped six energy piles. Once the measurements from the in situ campaign will be available, the model will be verified against on field experiments.

ACKNOWLEDGMENTS

The authors gratefully acknowledge the financial support of GeoGrid project PON03PE_00171_1. Furthermore the authors thank: Eng. F. Cavuoto as of Head Director of underground railway construction site of Piazza Municipio, Metropolitana di Napoli s.p.a. and SudMetro s.c.a.r.l.; Eng. G. Normino and Eng. P. Marotta from CRAVEB (Consorzio di Ricerca per l'Ambiente i Veicoli l'Energia e i Biocombustibili) for the technical support in the design and realization stages of the experimental set-up.

REFERENCES

Amatya, B., Soga, K., Bourne-Webb, P.J., Amis, T., Laloui, L. 2012. Thermo-mechanical behaviour of energy piles. *Géotechnique, 62(6)*: 503–519.

Amis, T. & Loveridge, F. 2014. Energy piles and other thermal foundations for GSHP, *The REHVA European HVAC Journal* 51(1).

Aversa, S. & Evangelista, A. 1993. Thermal Expansion of Neapolitan Yellow Tuff. *Rock Mech. Rock Engng. 26(4)*: 281–306.

Aversa, S., Evangelista, A., Scotto di Santolo, A. 2013. Influence of the subsoil on the urban development of Napoli. In Carlo Viggiani (ed.), *Geotechnical engineering for the preservation of monuments and historical sites*; *Proc. intern. symp., Napoli, 30–31 May 2013*. Rotterdam: Balkema.

Bourne-Webb, P.J., Amatya, B., Soga, K., Amis, T., Davidson, C., Payane, P. 2009. Energy pile test at Lambeth College, London: Geotechnical and thermodynamic aspects of pile response to heat cycles. *Géotechnique, 59*: 237–248.

Brandl, H. 2006. Energy foundations and other thermo-active ground structures. *Géotechnique 56*: 81–122.

Carotenuto, A., Massarotti, N., Mauro A. 2012. A new methodology for numerical simulation of geothermal down-hole heat exchangers. *Applied Thermal Engineering*, 48: 225–236.

Carotenuto, A., Ciccolella, M., Massarotti, N., Mauro A. 2016. Models for thermo-fluid dynamic phenomena in low enthalpy geothermal energy systems: A review. *Renewable and Sustainable Energy Reviews*, 60: 330–355.

Colombo, G. 2010. Il congelamento artificiale del terreno negli scavi della metropolitana di Napoli: valutazioni teoriche e risultati sperimentali. *Rivista Italiana di Geotecnica* 4.

Comsol. 2012. Comsol Multiphysics user manual version 4.3 *Palo Alto CA.*

Dupray, F., Laloui, L., Kazangba, A. 2014. Numerical analysis of seasonal heat storage in an energy pile foundation. *Computers and Geotechnics 55*: 67–77.

Jeong, S., Lim, H., Lee, K., Kim, J. 2014. Thermally induced mechanical response of energy piles in axially loaded pile groups. *Applied Thermal Engineering 71*: 608–615.

Laloui, L., Nuth, M., Vulliet, L. 2006. Experimental and numerical investigations of the behaviour of a heat exchanger pile. *Int. J. Numer. Anal. Meth. Geomech. 30*: 763–781.

Ozudogru, T.Y., Olgun, C.G., Arson, C.F. 2015. Analysis of friction induced thermo-mechanical stresses on a heat exchanger pile in isothermal soil. *Geotechnical and Geological Engineering* 33: 357–371.

Mottana, A., Campolunghi, M.P. 2010. Strutturazione di una banca dati in ambiente G.I.S. per lo sviluppo di impianti innovativi finalizzati alla gestione delle georisorse. *Report di ricerca si sistema elettrico. Accordo di programma Ministero dello Sviluppo Economico – ENEA*.

Salciarini, D., Tamagnini, C., Cinfrignini, E. 2012. Modellazione dei processi termo-idro-meccanici indotti in prossimità di pali geotermici. *IARG,Padova, 2–4 Luglio 2012.*

Salciarini, D., Ronchi, F., Cattoni, E., Tamagnini, C. 2015. Thermomechanical effects induced by energy piles operation in a small piled raft. *Int. J. Geomech.* 15(2).

Suryatriyastuti, M.E., Mroueh, H., Burlon, S. 2012. Understanding the temperature-induced mechanical behaviour of energy pile foundations. *Renewable and sustainable energy reviews, 16*: 3344–3354.

Viggiani, C., Rippa, F., 1998. Linea 1 della metropolitana di Napoli tratta Dante-Garibaldi. *Relazione Geologia e Geotecnica*.